CHAPTER 3

BLACKMAN DIAGRAMS AND ELASTIC-CONSTANT SYSTEMATICS

Hassel Ledbetter
Materials Science and Engineering Laboratory, National Institute of Standards and Technology, Boulder, Colorado, USA

Contents

ABSTRACT

We consider Blackman diagrams for various cubic materials. These diagrams, plots of reduced elastic-stiffness coefficients C_{12}/C_{11} versus C_{44}/C_{11}, show that materials with similar chemical bonding tend to fall in the same region of the diagrams. Such diagrams provide many uses. One important use is to enable determination of the complete cubic-symmetry $C_{ij} - C_{11}$, C_{12}, C_{44} from the quasi-isotropic (polycrystal) elastic constants. The diagram gives information about elastic anisotropy, departures from central interatomic forces, and lattice instabilities. Examples considered include b.c.c. metals, f.c.c. metals, diamond-cubic elements, alkali halides, oxides, 8–N compounds, carbides, semiconductors, and Fe–Cr–Ni alloys (austenitic stainless steels).

3.1. INTRODUCTION

In 1938, in considering cubic-symmetry materials, Blackman [1] discovered that plotting the reduced elastic-stiffness coefficients C_{12}/C_{11} versus C_{44}/C_{11} led to a surprising result: materials with similar chemical bonding fall into the same region of the diagram, despite large differences in their absolute stiffnesses! (Here C_{ij} denote the usual reduced-index Voigt elastic stiffnesses, for cubic symmetry three independent ones: C_{11}, C_{12}, C_{44}.) Blackman also described how his diagram contains the usual mechanical-stability criteria. As described here, the diagram contains much more information not

Handbook of Elastic Properties of Solids, Liquids, and Gases, edited by Levy, Bass, and Stern
Volume II: Elastic Properties of Solids: Theory, Elements and Compounds, Novel Materials, Technological Materials, Alloys, and Building Materials

ISBN 0-12-445762-2 / $35.00

evident to Blackman because of the few available reliable monocrystal C_{ij} measurements. (His original diagram contained only 18 points.)

First we consider the mechanical-stability conditions. Blackman gave four:

(a) $C_{44} > 0$,
(b) $C_{11} - C_{12} > 0$,
(c) $C_{11} > 0$,
(d) $C_{11} + C_{12} + 2C_{44} > 0$.

From conditions (a) and (d), it follows that

(e) $C_{11} + 2C_{12} > 0$.

In a cubic crystal, C_{44} corresponds physically to shear resistance on a (100) plane, $C_{11} - C_{12}$ to shear resistance on a (110) plane, and $(C_{11} + 2C_{12})/3$ to the bulk modulus B representing resistance to volume change $\Delta V/V$ caused by hydrostatic pressure P:

$$\Delta V/V = -P/B \tag{3.1}$$

a special case of Hooke's law.

3.2. BLACKMAN DIAGRAMS

Figure 3.1 shows a general Blackman diagram where the three bold lines correspond to the stability conditions (a), (b), and (e). As described below, almost all materials fall in region 1. Thus, we shall focus only on this region. Materials in region 2 are exceptionally rare. Now that the FeS_2 case has been resolved [2], no materials are known in region 3. Likewise, none were reported for region 4.

Figure 3.2 shows a region-1 diagram to which are added lines of constant elastic anisotropy

$$A = 2C_{44}/(C_{11} - C_{12}) \tag{3.2}$$

Obviously, $A = \infty$ corresponds to $C_{11} = C_{12}$ and $A = 0$ to $C_{44} = 0$. Figure 3.2 also shows a line corresponding to central interatomic forces, which require the Cauchy

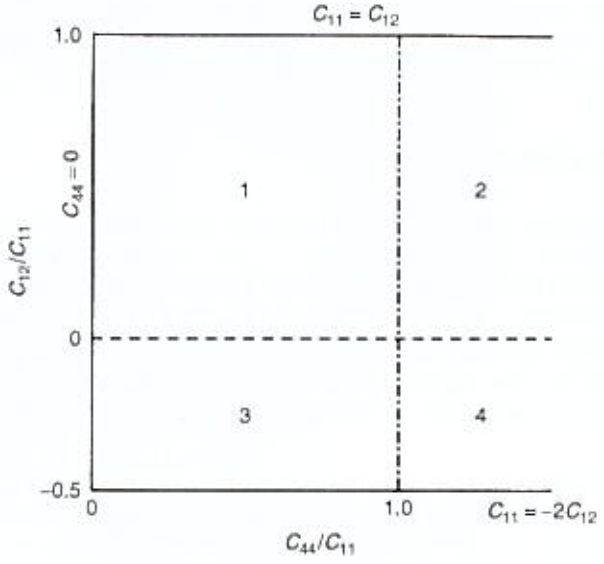

Fig. 3.1. General Blackman diagram showing mechanical-stability limits.

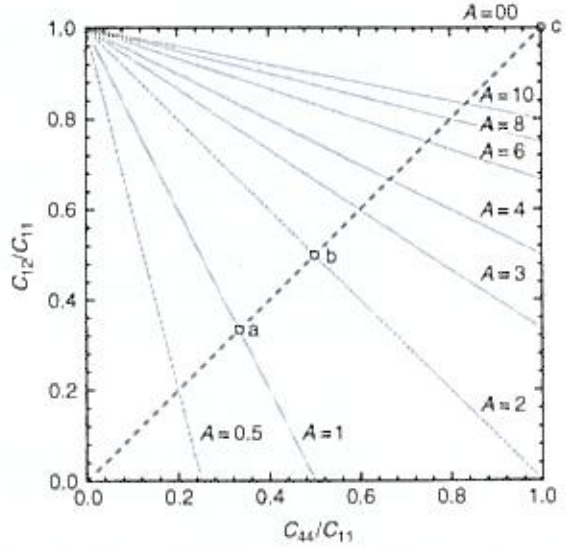

Fig. 3.2. Blackman diagrams showing lines of constant Zener elastic anisotropy $A = 2C_{44}/(C_{11} - C_{12})$. Also shown is the central-force line corresponding to $C_{12} = C_{44}$, an important factor in theoretical calculations of the C_{ij}.

relationship $C_{12} = C_{44}$. Thus, if a material is both isotropic and interatomic, forces are central: it falls at point a. Face-centered-cubic central-force crystals fall near point b because a nearest-neighbor model calculation for the f.c.c. case gives $A = 2$[3]. Central-force nearest-neighbor-interaction-only b.c.c. crystals fall at point c, $A = \infty$. It is well known that the most anisotropic crystals are usually b.c.c. Clearly, the effect of second-nearest-neighbor interactions is to reduce A to a finite value.

Figure 3.3 shows the diagram for f.c.c. elements. Except for iridium, rhodium, and thallium, interatomic forces are noncentral. Except for cerium and plutonium, all departures are toward the $C_{12} > C_{44}$ side. Plutonium is the most anisotropic f.c.c. element.

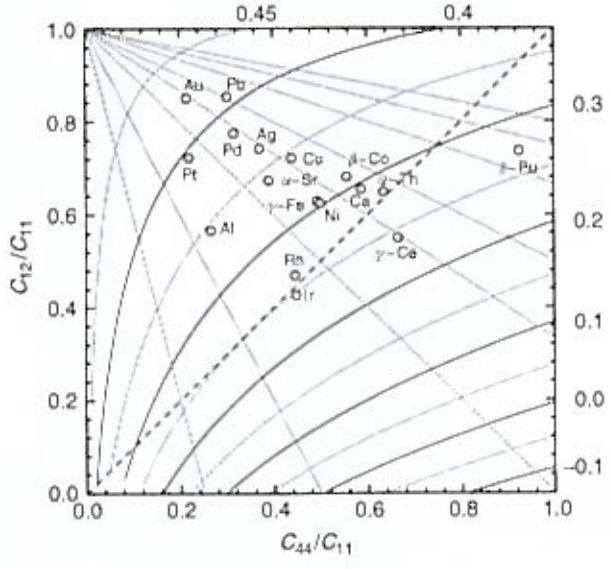

Fig. 3.3. Blackman diagram for face-centered-cubic elements.

The elements tend to cluster along $A = 3$ rather than along $A = 2$, as predicted by the simplest models. Face-centered cubic elements tend to cluster in the upper-left quadrant. Ledbetter [4] considered f.c.c. elements and alloys that fall in the upper-right quadrant and gave an interatomic-force-constant argument for their "chemical" (not mechanical) instability, which leads to phase transformations.

Figure 3.3 also shows curves of constant Poisson ratio ν, obtained by averaging over direction using Kröner's theory [5]. These Poisson-ratio curves show why the lower-right quadrant is usually empty. It corresponds to a very low, or even negative, Poisson ratio. These curves emphasize that materials with very different chemical bonding can have a similar Poisson ratio, and they show that ν increases as C_{12} increases. We can understand this as follows. For a cubic crystal in the [100] direction, the Poisson ratio is [6]

$$\nu_{100} = -S_{12}/S_{11} = C_{12}/(C_{11} + C_{12}) \tag{3.3}$$

Here, the S_{ij} denote the elastic compliances. In the Blackman diagram, ν represents the average of Eq. 3.3 over all directions. The strong dependence on C_{12} survives the averaging.

Figure 3.4 shows the diagram for b.c.c. elements. For lack of measured C_{ij}, Blackman believed that b.c.c. elements all fall in the upper-right quadrant. But there are two clusters: alkali metals in the upper right and transition metals (d-shell-bonded) mainly in the lower left. Except for iron (perhaps because of its magnetism), the transition metals show anisotropies of about one or less. All the alkali metals show high elastic anisotropy, caused by their relatively low $C_{11} - C_{12}$ values. Their proximity to the stability criterion, $(C_{11} - C_{12}) > 0$, suggest their instability. Indeed, at low temperatures, both lithium and sodium transform to either f.c.c. or c.p.h. crystal structures [7].

Figure 3.5 shows the diagram for diamond-cubic elements. All three lie near $C_{44}/C_{11} = 0.5$ and show relatively low Poisson ratios, especially diamond where bond-bending force constants are relatively large compared with bond-stretching force constants. Of three suggested force-constant models, clearly Keating's works best.

Moving to compounds, Figure 3.6 shows the diagram for 22 alkali halides, which cluster in the lower-left quadrant. Most all these compounds are considered to contain mainly ionic (heteropolar) bonding. The oxides shown in Figure 3.7 are also usually

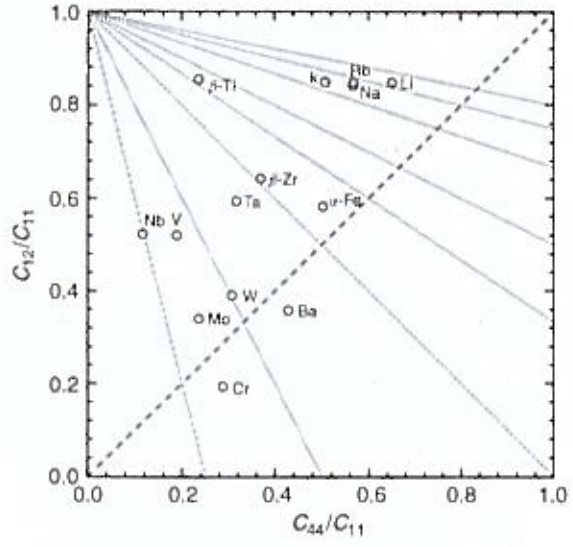

Fig. 3.4. Blackman diagram for body-centered-cubic elements.

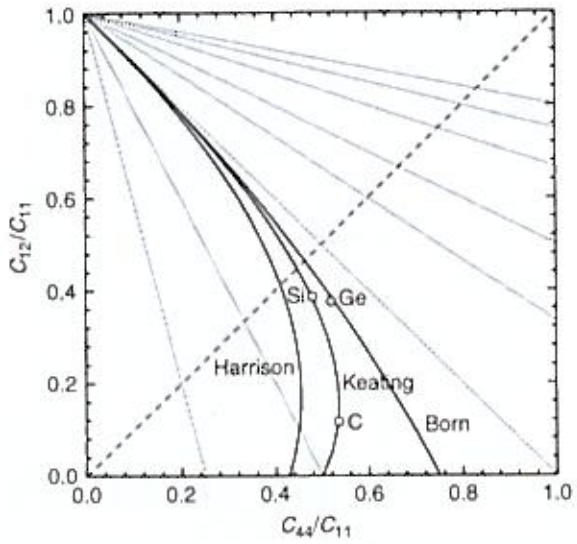

Fig. 3.5. Blackman diagram for diamond-cubic elements. Also shown are curves representing three force-constant models.

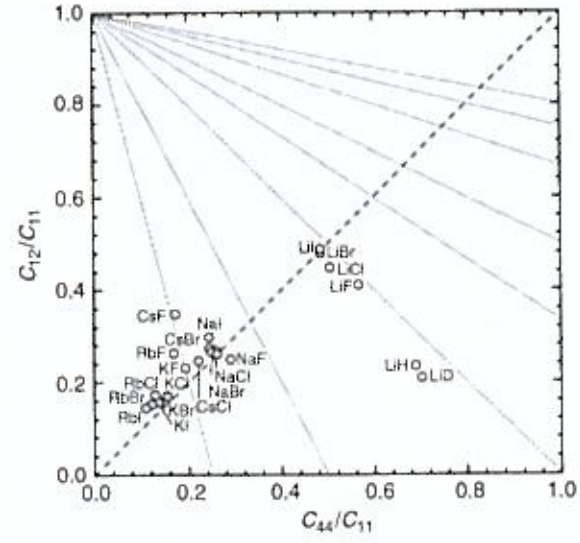

Fig. 3.6. Blackman diagram for alkali halides.

considered ionic-bond compounds. In Figure 3.6, especially noteworthy is that the lithium halides, near the diagram's center, fall far from the sodium, potassium, rubidium halides, which form a relatively tight cluster with a very different elastic anisotropy, ~0.5 versus ~2. This suggests that the lithium halides differ strongly in their chemical bonding compared with the sodium, potassium, and rubidium halides. The lithium halides are much stiffer than the sodium, potassium, and rubidium halides, especially in their shear stiffness C_{44}. Ionic sizes play a key role. As described by Pauling [8], in these crystal structures, in the lithium-cation case, anion–anion contact occurs along [110] directions because the lithium ion is so small. Thus, anion–anion repulsive forces arise, and the lithium halides are elastically stiffer than their sodium, potassium, rubidium counterparts where the anion–anion interaction is much weaker.

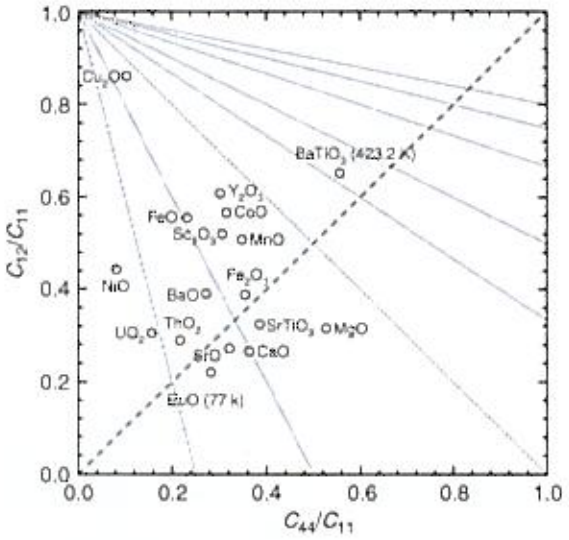

Fig. 3.7. Blackman diagram for oxides.

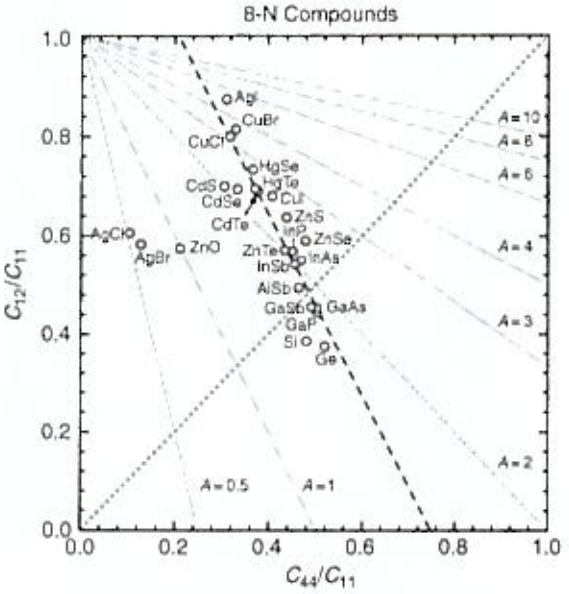

Fig. 3.8. Blackman diagram for covalent (homopolar) compounds.

Covalent (homopolar) compounds are shown in Figure 3.8. They tend to cluster along a line represented approximately by

$$C_{11} = \tfrac{2}{3}(C_{12} + 2C_{44}) \tag{3.4}$$

For details on these compounds, see Chapter 16 in this volume.

Transition-metal carbides, which form a rocksalt crystal structure, are shown in Figure 3.9. Like the ionic compounds, they cluster in the lower-left corner. Pauling [9] considered these carbides to contain six resonating covalent bonds. As described in detail by Cottrell [10], the $(x^2 - y^2)$ and $(3z^2 - r^2)$ 3d transition-metal orbitals interact strongly with carbon's sp^3 hybrid orbitals. Cottrell also emphasized that these

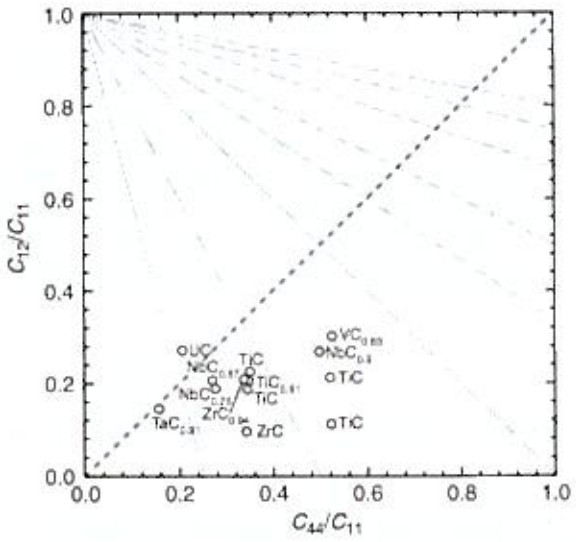

Fig. 3.9. Blackman diagram for transition-metal carbides.

compounds contain opportunities for six covalent bonds, unlike the semiconductors in Figure 3.8, which contain four covalent bonds and a tetrahedral (zincblende) crystal structure. Thus, covalent compounds with different coordination numbers fall in different regions of the Blackman diagram. For NbC, Ledbetter and coworkers [11] gave a detailed discussion of covalent-ionic-metallic bonding, including reference to the Blackman diagram. References to the results plotted in Figure 3.9 occur in Toth [12].

We could show Blackman diagrams for other sets of materials. But, the above examples illustrate the principal features. Also, we shall not show effects of temperature, pressure, alloying, phase transformations, or other variables, which can be studied usefully with these diagrams.

As a practical example, we consider austenitic steels (Fe–Cr–Ni and related alloys), which are face-centered cubic. Figure 3.10 shows the diagram, based on C_{ij}

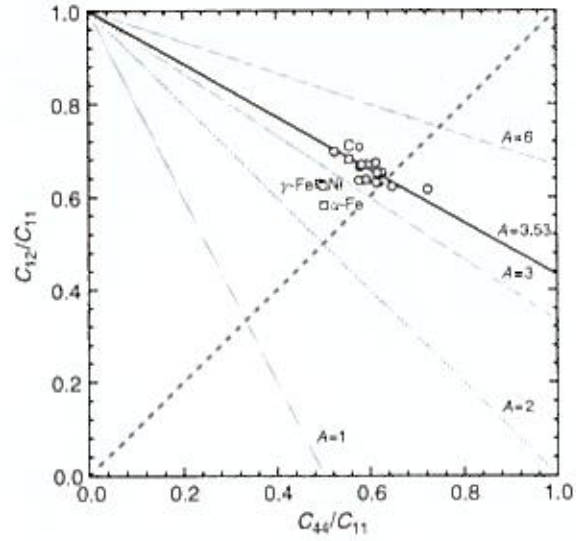

Fig. 3.10. Blackman diagram for austenitic steels (f.c.c. Fe–Cr–Ni alloys).

summarized by Ledbetter [13]. The diagram also contains points for nickel, cobalt, α-iron, and γ-iron. We observe a surprising result: Fe–Cr–Ni alloys tend to fall along a line of constant elastic anisotropy, $A = 2C_{44}/(C_{11} - C_{12}) = 3.53$. This observation provides enormous utility. It means that we can estimate the three monocrystal C_{ij} from the two polycrystal elastic constants by using an averaging theory such as Kröner's [5] inversely. Good polycrystals are much more available than good monocrystals. In some cases, obtaining monocrystals is difficult, if not impossible. For example, if a phase transformation occurs, preparing a monocrystal of the low-temperature phase is usually very difficult. But, preparing a good polycrystal is usually trivial.

3.3. SUMMARY

In summary, Blackman diagrams contain many features, which include the following:

1. Clustering of materials with similar interatomic bonding, independent of their absolute elastic stiffnesses,
2. Proximity of materials to the mechanical-stability bounds,
3. Elastic-anisotropy trends,
4. Effective Poisson ratio, which reflects interatomic-bonding type,
5. Ability to estimate C_{12}/C_{11} and C_{44}/C_{11} ratios for materials not yet measured,
6. Ability to estimate the monocrystal C_{ij} from the polycrystal elastic constants,
7. Ability to identify suspect C_{ij} measurements,
8. Ability to show effects of variables of temperature, pressure, composition, phase transformations, and so on.

References

1. Blackman, M. (1938). *Proc. Roy. Soc. Lond.* **164**: 62.
2. Simmons, G., and Birch, F. (1963). *J. Appl. Phys.* **34**: 2736.
3. Ledbetter, H. (1976). *Z. Naturforsch.* **31a**: 1539.
4. Ledbetter, H. Elastic constants and instability in face-centered-cubic metals, to be published.
5. Kröner, E. (1958). *Z. Phys.* **151**: 504.
6. Nye, J. (1960). *Physical Properties of Crystals*, p. 147. London: Oxford U.P.
7. Barrett, C. (1956). *Acta Crystallogr.* **9**: 671.
8. Pauling, L. (1960). *Nature of the Chemical Bond*, p. 520. Ithaca: Cornell U.P.
9. Ref. 8, p. 435.
10. Cottrell, A. (1995). *Chemical Bonding in Transition-Metal Carbides*, London: Institute of Materials.
11. Ledbetter, H., Chevacharoenkul, S., and Davis, R. (1986). *J. Appl. Phys.* **60**: 1614.
12. Toth, L. (1971). *Transition-Metal Carbides and Nitrides*, p. 146. New York: Academic.
13. Ledbetter, H. (1984). *Phys. Status Solidi (a)* **85**: 89.